HEPATOLOGY

HEPATOLOGY, VOL. 68, NO. 3, 2018



# Sphingosine Kinase 1 Promotes Liver Fibrosis by Preventing miR-19b-3p-Mediated Inhibition of CCR2

Tian Lan,[1-3*] Changzheng Li,[1*] Guizhi Yang,[1*] Yue Sun,[1-3] Lihang Zhuang,[1-3] Yitao Ou,[1] Hui Li,[5] Genshu Wang,[5] Tatiana Kisseleva,[4] David Brenner,[4] and Jiao Guo[1-3]

**Chronic liver disease mediated by activation of hepatic stellate cells (HSCs) and Kupffer cells (KCs) leads to liver fibrosis. Here, we aimed to investigate the molecular mechanism and define the cell type involved in mediating the sphingosine kinase (SphK)1-dependent effect on liver fibrosis. The levels of expression and activity of SphK1 were significantly increased in fibrotic livers compared with the normal livers in human. SphK1 was coexpressed with a range of HSC/KC markers including desmin, α-smooth muscle actin (α-SMA) and F4/80 in fibrotic liver. Deficiency of SphK1 (SphK1$^{-/-}$) resulted in a marked amelioration of hepatic injury, including transaminase activities, histology, collagen deposition, α-SMA and inflammation, in $CCl_4$ or bile duct ligation (BDL)-induced mice. Likewise, treatment with a specific inhibitor of SphK1, 5C, also significantly prevented liver injury and fibrosis in mice induced by $CCl_4$ or BDL. In cellular levels, inhibition of SphK1 significantly blocked the activation and migration of HSCs and KCs. Moreover, SphK1 knockout in KCs reduced the secretion of CCL2, and SphK1 knockout in HSCs reduced C-C motif chemokine receptor 2 ([CCR2] CCL2 receptor) expression in HSCs. CCL2 in SphK1$^{-/-}$ mice was lower whereas microRNA-19b-3p in SphK1$^{-/-}$ mice was higher compared with wild-type (WT) mice. Furthermore, microRNA-19b-3p downregulated CCR2 in HSCs. The functional effect of SphK1 in HSCs on liver fibrosis was further strengthened by the results of animal experiments using a bone marrow transplantation (BMT) method. *Conclusion:* SphK1 has distinct roles in the activation of KCs and HSCs in liver fibrosis. Mechanistically, SphK1 in KCs mediates CCL2 secretion, and SphK1 in HSCs upregulates CCR2 by down-regulation of miR-19b-3p. (HEPATOLOGY 2018; 68:1070-1086).**

Hepatic fibrosis is characterized by excess accumulation of extracellular matrix that follows chronic liver injury.[1] Advance fibrosis is characterized by accumulation of activated α-smooth muscle actin (α-SMA)-positive periportal and perisinusoidal myofibroblasts that lead to scar formation composed of collagens.[1] Ongoing inflammation often results in massive fibrosis and finally cirrhosis, which is accompanied by architectural distortion of the hepatic vasculature and sets the stage for hepatic

*Abbreviations: ALT, alanine aminotransferase; AST, asparate aminotransferase; α-SMA, α-smooth muscle actin; BDL, bile duct ligation; BM, bone marrow; BMSCs, bone marrow-derived mesenchymal stem cells; BMT, bone marrow transplantation; CCL2, C-C motif chemokine ligand 2; CCR2, C-C motif chemokine receptor 2; Col1α1, collagen type I alpha 1; ECM, extracellular matrix; HSCs, hepatic stellate cells; KCs, kupffer cells; NPs, nanoparticles; SphK, sphingosine kinase; S1P, sphingosine-1-phosphate; TGF-βR2, TGF-β receptor 2; TIMP-1, TIMP metallopeptidase inhibitor 1; TGF-β1, transforming growth factor-β; WT, wild-type.*

*Received November 9, 2017; accepted March 9, 2018.*

*Additional Supporting Information may be found at onlinelibrary.wiley.com/doi/10.1002/hep.29885/suppinfo*

*Supported by grants from Key Project of National Natural Science Foundation of China (81530102); the Science and Technology Planning Project of Guangdong Province (2017A020211007), China; and the Key Project of Natural Science Foundation of Guangdong Province (2016A030311014), China.*

**These authors contributed equally to this work.*



*View this article online at wileyonlinelibrary.com.*

*DOI 10.1002/hep.29885*

*Potential conflict of interest: Nothing to report.*

decompensation, primary liver cancer, and death.[2] Upon liver injury, hepatic stellate cells (HSCs), the major collagen-synthesizing cells in the liver, become activated and transdifferentiate into myofibroblast-like cells that proliferate faster and display enhanced chemotaxis, survival and collagen production.[1] HSCs also play an important role in linking hepatic inflammation to fibrogenesis.[3] HSC activation is driven by multiple mediators, such as chemokines, reactive oxygen species, growth factor, matrix stiffness, matricellular proteins and damage-associated molecular patters, which are also secreted by neighboring cells and signals to drive scarring by HSCs in an autocrine and/or paracrine fashion.[4,5] However, a limitation of the current anti-fibrotic therapy is that medicinal candidates cannot specifically target HSCs. Therefore, understanding the molecular mechanism of fibrogenesis is important for the development of effective antifibrotic therapies.

Macrophages are key drivers of fibrogenesis and found in close proximity with collagen-producing myofibroblasts. A crucial step in the initiation of liver fibrosis is a strong inflammatory response. Liver resident macrophages (Kupffer cells [KCs]) become activated and release proinflammatory and profibrotic mediators that activate quiescent HSCs into myofibroblasts producing α-SMA.[6,7] Several studies have emphasized the crucial role of infiltrating monocytes/macrophages for the progression of liver inflammation and fibrosis in experimental mouse models[8,9] and in patients with liver cirrhosis.[10] KCs are greatly augmented by an overwhelming number of infiltrating monocytes upon acute or chronic liver injury. Chemokines have been identified as central regulators of liver fibrosis. In conditions of liver damage, C-C motif chemokine receptor (CCR)2 and its ligand, monocyte chemotactic protein-1/C-C motif chemokine ligand 2 (monocyte chemotactic protein-1/CCL2), promote monocyte subset infiltration into the liver.[9,11,12] The expression of CCL2 is associated with infiltration of monocytes.[13] The functional relevance of the CCL2-CCR2 pathway has been extensively confirmed in various experimental models of liver fibrosis using genetic deletion of CCL2, CCR2 or pharmacological inhibition of CCL2, resulting in attenuation of liver fibrosis in mice.[9,11,14,15]

Sphingosine-1-phosphate (S1P) is a pleiotropic lipid mediator that acts either on G protein-couple S1P receptors on the cell surface or via intracellular target sites. S1P is converted from sphingosine by two isoforms of sphingosine kinases (SphK1 and SphK2).[16] Among the chemokines and inflammatory mediators known to exert potent cellular chemotactic effects, the S1P has been recognized as an important regulator of fibrosis in lung, kidney, heart and skin.[17-21] Recent reports showed that a SphK1/S1P/S1PR signaling axis was involved in liver injury and fibrosis.[22-25] SphK inhibitor can reduce angiogenesis in fibrotic mice[24] and block the differentiation from bone marrow-derived mesenchymal stem cells (BMSCs) to myofibroblasts during liver injury,[26] suggesting that targeting SphK might be a therapy in the treatment of liver fibrosis. However, the protective effects of SphK1 knockout *in vivo* and cell-type-specific roles of the SphK1 in the pathogenesis of liver fibrosis have not been defined yet.

Therefore, the current study aimed to characterize the cell-type-specific contribution of SphK1 activation during liver fibrosis. We address the profibrotic roles of SphK1 by combination of SphK1 knockout mice and bone marrow transplantations (BMTs). The current study showed that knockout of SphK1 in mice or inhibition of SphK1 activity attenuates liver fibrosis in mice. We demonstrate that SphK1 in HSCs, plays a crucial role during liver fibrosis. Together, these results represent direct experimental evidence that SphK1 is a therapeutic target for liver fibrosis.

## ARTICLE INFORMATION:

From the [1]Guangdong Pharmaceutical University, Guangzhou, China; [2]Guangdong Metabolic Disease Research Center of Integrated Chinese and Western Medicine, Guangzhou, China; [3]Joint Laboratory of Guangdong, Hong Kong and Macao on Glycolipid Metabolic Diseases, Guangzhou, China; [4]Department of Medicine, University of California San Diego, La Jolla, CA; and [5]Department of Hepatic Surgery and Liver transplantation Center of the Third Affiliated Hospital, Sun Yat-sen University, Guangzhou, China.

## ADDRESS CORRESPONDENCE AND REPRINT REQUESTS TO:

Jiao Guo, M.D., Ph.D.
Guangdong Pharmaceutical University
280 Wai Huan Dong Road
Guangzhou 510006, China
E-mail: guoj@gdpu.edu.cn
Tel: +86 (20) 39352818

# Materials and Methods

## ANIMALS

Specific pathogen-free C57BL/6 mice were obtained from the Medical Laboratory Animal Center (Guangzhou, China). SphK1 knockout (SphK1$^{-/-}$) mice were C57BL/6 background and donated by Richard Proia of National Institute of Health. PCR screening of SphK1 was performed using the following primers: SphK1-1:5′-TGTCACCCATGAACCTGCTGTCCCTGCACA-3′; SphK1-2:5′-AAUGGUUCAAGCUGCTT-3′. SphK1-3: 5′-TCGTGCTTTACGGTATCGCCGCTCCCGATT-3′; All mice received human care and animal experiments were approved by the University Committee on Use and Care of Animals of the Guangdong Pharmaceutical University, Guangzhou, China.

## miRNA MICROARRAY

Total RNA including miRNA was isolated with TRIZOL Reagent (Invitrogen, Massachusetts, USA) from liver tissues treated with $CCl_4$ or corn-oil (vehicle control) for 6 weeks, following the manufacturer's instructions. RNA quantity and quality were determined using a nanodrop (Thermo Scientific, Massachusetts, USA) and Bioanalyzer (Agilent Inc., California, USA). Total RNA (100 ng) was labelled with desalted Cy3 using an miRNA Complete Labeling and Hyb kit (Agilent) and then hybridized to an Agilent miRNA expression microarray in accordance with the manufacturer's instructions. A Sureprint G3 Mouse miRNA Microarray (Release 19.0, 8 x 60K; Agilent). For microarray analysis, raw data were first filtered by a flag signal detected in all samples. Filtered raw data were processed using the Limma Bioconductor package (http://www.bioconductor.org/) in the R statistical environment (http://www.r-project.org/). After quantile normalization of data, miRNAs with twofold or greater differential expression were identified, with *P*-values of $< 0.05$ being considered statistically significant.

## BONE MARROW TRANSPLANTATION

Bone marrow transplantation (BMT) was performed as described previously. Briefly, mice were macrophage depleted by injection of liposomal clodronate (10 $\mu$l/g, Clodrosome, TN,USA), followed by lethal irradiation with 10.8 Gy and intravenous injection of 1 x $10^7$ bone marrow (BM) cells from donor mice. Successful BM transplantation was confirmed by the absence of SphK1-positive macrophages in the liver (Supporting Fig. S4).

## CHEMOKINE ARRAY

Hepatic chemokine secretion profile was screened using a mouse chemokine array kit (RayBiotech, Georgia, USA) following manufacturer's instructions. The array consists of 25 different mouse chemokine antibodies spotted in duplicate onto membranes. Array membranes were incubated for 1 hour in blocking buffer and then incubated overnight with liver protein lysates. The membranes were washed and incubated with streptavidin-horseradish peroxidase and Chemi Reagent Mix. The intensity of each chemokine spot was determined by Image J software and represented as relative expression compared with control.

## LUCIFERASE REPORTER ASSAY

Plasmids of GP-miRGLO (Genepharma, Shanghai, China) containing either the WT or mutated CCR2 mRNA 3′UTR were cotransfected with miR-19b-3p mimic or negative control in primary HSCs. After transfection for 48 hours, the cells were lysed for luciferase activity with a Dual-Luciferase® Reporter Assay System (Promega, Madison, WI, USA), and firefly luciferase activity was normalized to Renilla luciferase activity.

## ADDITIONAL MATERIALS AND METHODS

A detailed description of methodologies used in this study can be found in the Supporting Materials and Methods.

## STATISTICAL ANALYSIS

Values were expressed as mean ± standard deviations. Statistical differences between two groups were analyzed by the unpaired Student *t* test with a two-tailed distribution. Differences between multiple groups of data were analyzed by one-way ANOVA with Bonferroni correction (Graph Pad Prism 6.0, San Diego, CA, USA). A *P* value $<0.05$ was considered statistically significant.

# Results

## SPHK1 SIGNALING IS ACTIVATED IN HUMAN AND RODENT LIVER FIBROSIS

We initially examined SphK1 levels in human liver fibrotic tissue in HBV-induced cirrhosis and primary biliary cirrhosis. SphK1 mRNA expression increased significantly in liver fibrosis biopsies (Fig. 1). Immunohistochemical analyses revealed that hepatic SphK1 expression was higher in patients with cirrhosis than healthy control (Fig. 1A). The fibrotic areas were represented by sirius red staining and activated HSCs were represented by α-SMA positive staining. Furthermore, SphK1 expression was accumulated in hepatic collagen area (Fig. 1A). Moreover, α-SMA mRNA levels were higher in cirrhotic livers than in healthy livers. As expected, the mRNA levels of SphK1 were elevated in cirrhotic livers (and positively correlated with mRNA levels of α-SMA Fig. 1B). Consistently, the protein expression and activity of SphK1 was also markedly increased in cirrhotic livers (Fig. 1C,D). We also observed elevation of SphK1 expression and activity in a mouse model of liver fibrosis induced by $CCl_4$ (Fig. 1E,F). Interestingly, $CCl_4$-injured mouse liver displayed SphK1 staining in cells with a myofibroblast-like morphology in fibrotic tissue (Fig. 1E). These data indicate that SphK1 is upregulated in cirrhotic livers, raising the hypothesis that the activation of SphK1 signaling plays a role in the activation of HSCs and the progression of liver fibrosis.

To define the cellular distribution of SphK1, we performed immunofluorescence double staining of SphK1 with desmin (a marker for HSCs), α-SMA (a marker for activated HSCs), F4/80 (a marker for

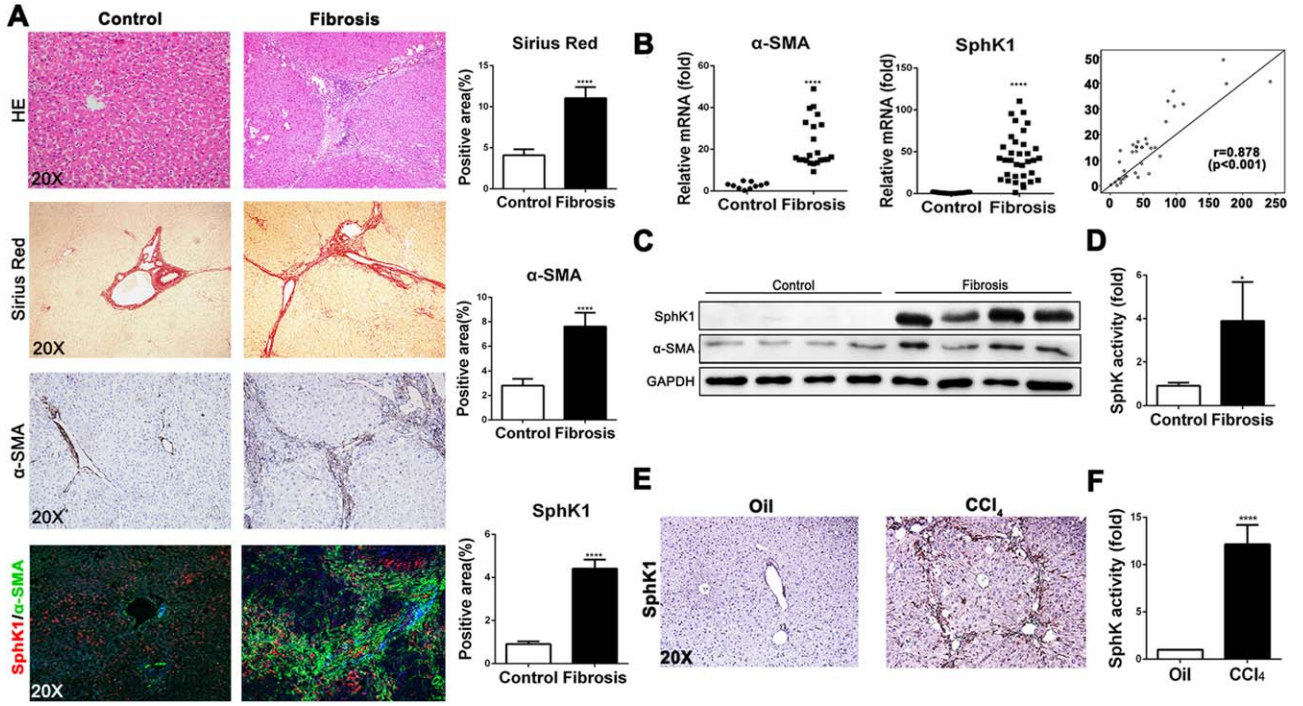


**FIG. 1.** Increased levels of SphK1 are associated with human and rodent liver fibrosis. (A) Paraffin-embedded sections of liver tissues from healthy controls (Control, n=10) and patients with fibrosis (Fibrosis, n=30) were stained with H&E, Sirius Red, and immunohistochemical staining of α-SMA and SphK1. The positive staining areas were measured by Image J software. (B) Transcript levels of SphK1 and α-SMA in healthy individuals or patients with cirrhosis, and the positive correlation of hepatic SphK1 mRNA with α-SMA. Data were shown as box and whisker plot. Statistical significance of differences between healthy individuals and patients with cirrhosis was determined by unpaired two-sample Student *t*-test (n = 20 or 35 each). (C) Representative bands of SphK1 in healthy and fibrotic livers (n=4 for each) was analyzed by Western blotting assay. (D) Activity of SphK1 was measured with LC-MS/MS analysis (n = 8). (E) IHC staining for SphK1 on the liver sections from representative mice treated with vehicle or $CCl_4$ (1 ml/kg body weight, intraperitoneal injection, twice a week, for 6 weeks). (F) Activity of SphK1 was measured with LC-MS/MS analysis in mice. Data are presented as means ± SD $^{*}P<0.05$; $^{**}P<0.01$; $^{****}P<0.0001$ versus Control.

KCs), or albumin (a marker for hepatocytes), we found that SphK1 was expressed in HSCs and KCs, but not in hepatocytes. Furthermore, SphK1 was dramatically upregulated and primarily expressed in HSCs after chronic liver injury (Supporting Fig. S1).

## DEFICIENCY OF SphK1 PROTECTS AGAINST LIVER FIBROSIS IN MICE

On the basis of the increase in SphK1 expression in fibrotic liver, we then examined the role of SphK1 signaling in hepatic fibrosis in SphK1 knockout ($SphK1^{-/-}$) mice subjected to $CCl_4$ or bile duct ligation (BDL). Mice were repetitively exposed to $CCl_4$ for 6 weeks. Hematoxylin and eosin (H&E) and sirius red staining assays revealed that SphK1 deficiency inhibited $CCl_4$-induced liver injury and fibrosis as compared with controls. Consistently, deficiency of SphK1 notably attenuated upregulation of α-SMA and collagen type 1 (Col1α1), the most abundant extracellular matrix (ECM) protein in the fibrotic liver. Similarly, the immunostaining of CD68, a well-established marker of activated macrophage marker, was also decreased in $SphK1^{-/-}$ mouse liver (Fig. 2A). The hepatic mRNA levels of fibrogenic genes (α-SMA, Col1α1, TGF-β1, TIMP-1 and PDGF) were reduced in $CCl_4$-injured $SphK1^{-/-}$ mice (Fig. 2B). Consistently, the hepatic mRNA levels of inflammatory genes (F4/80, TNF-α and IL-1β) were also decreased in $CCl_4$-injured $SphK1^{-/-}$ mice (Fig. 2C). The low level of fibrosis observed in SphK1-/- mice may have been a result of attenuation of the injury process. As expected, the serum levels of alanine aminotransferase (ALT) and aspartate aminotransferase (AST) were significantly diminished in $SphK1^{-/-}$ mice, indicative of improvement of liver damage (Fig. 2D). In addition, immunoblotting results showed that the expression of α-SMA and collagen I was reduced in fibrotic liver from $SphK1^{-/-}$ mice than WT mice (Fig. 2E).

To further analyze the role of SphK1 in liver fibrosis, we employed the BDL mouse model of liver fibrosis, another well-established model. SphK1 deficiency attenuated the development of liver fibrosis in BDL-operated mice for 15 days, as evidenced by histopathological improvement and the changes in Sirius Red staining. Repression of α-SMA and CD68 staining was observed in BDL-operated $SphK1^{-/-}$ mice compared with WT mice (Fig. 3A). The hepatic mRNA levels of fibrotic and inflammatory factors were also suppressed in $SphK1^{-/-}$ mice operated by BDL for 15 days (Fig. 3B,C), correlated with decreased serum levels of ALT and AST (vs WT mice, [Fig. 3D])

To validate the biological impact of SphK1 deficiency, we also used mouse models of acute hepatitis induced by a single injection of $CCl_4$ or BDL for 5 days, respectively. Liver inflammatory cell infiltration and hepatocyte necrosis were increased in WT mice subjected by $CCl_4$ or BDL. In concordance, the expression of SphK1 was increased in damaged liver (Supporting Fig. S2A). Consistently, the expression of α-SMA and CD68 was diminished in $SphK1^{-/-}$ mice operated by BDL for 5 days (Supporting Fig. S2B). The qRT-PCR assays for fibrogenic and inflammatory factors confirmed that SphK1 deficiency inhibited fibrogenic and inflammatory gene induction (Supporting Fig. S2C,D). Additionally, liver function was improved in $SphK1^{-/-}$ mice (Supporting Fig. S2E), suggesting that SphK1 deficiency also has an inhibitory effect on the early pathologic event leading to the liver injury and fibrosis. Taken together, all of these results demonstrate that SphK1 mediates the activation of HSCs and KCs, contributing to the initiation and progression of liver fibrosis.

## SphK1 SIGNALING IS REQUIRED FOR HSC ACTIVATION

We hypothesized that the increased SphK1 may regulate HSC activation. Next, we used two methods to inhibit SphK1 signaling: blockage of SphK1 using a specific inhibitor of SphK1 (5C) and knockdown of SphK1 by siRNA. In the current study, LX-2 (a human HSC line with key features of activated HSCs despite limitations due to immortalization) was treated with SphK1 siRNA or 5C. qRT-PCR analysis demonstrated that SphK1 siRNA or 5C significantly reduced the mRNA levels of profibrogeic genes (α-SMA, Col1α1, TGF-β1, TIMP-1 and PDGF) in LX-2 cells (Fig. 4A), with almost 90% downregulation of SphK1 mRNA by SphK1 silencing (Fig. 4B). We also found that SphK1 activity was significantly inhibited by 5C or SphK1 siRNA (Fig. 4C). Consistently, SphK1 siRNA or 5C remarkably downregulated α-SMA in LX-2 cells (Fig. 4D). In contrast, overexpression of SphK1 in LX-2 cells transfected with SphK1 plasmid further enhance α-SMA expression (Fig. 4E). These results suggested that SphK1 promotes liver fibrosis involved in the regulation of HSC activation.

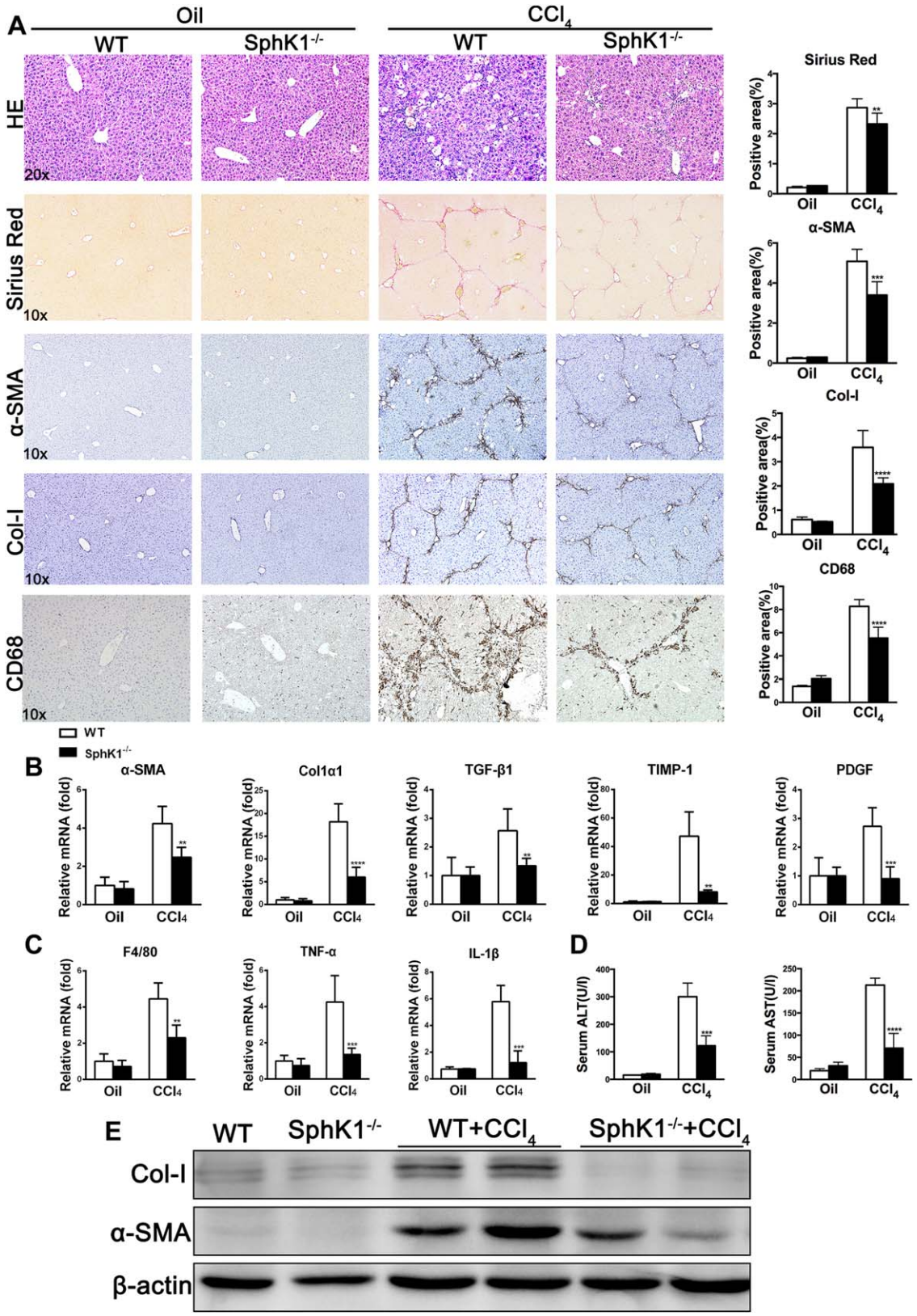


**FIG. 2.** Hepatic fibrosis is attenuated in SphK1$^{-/-}$ mice after $CCl_4$ treatment. Livers were obtained from mice after 12 intraperitoneal injections of $CCl_4$ treatment. (A) Representative images of H&E, Sirius red and IHC staining for α-SMA, collagen type 1 and CD68 were done on the liver tissues of WT and SphK1$^{-/-}$ mice. Quantification of positive staining areas were measured by Image J software. Hepatic mRNAs of fibrogenic genes (B) and inflammatory genes (C) were measured by qRT-PCR assays in WT and SphK1$^{-/-}$ mice induced by $CCl_4$. (D) Liver function was assessed by serum levels of ALT and AST in mice. (E) Immunoblottings analyses of α-SMA and collagen I expression in the mouse liver. $^{**}P<0.01$; $^{***}P<0.001$; $^{****}P<0.0001$ versus WT mice treated with $CCl_4$.

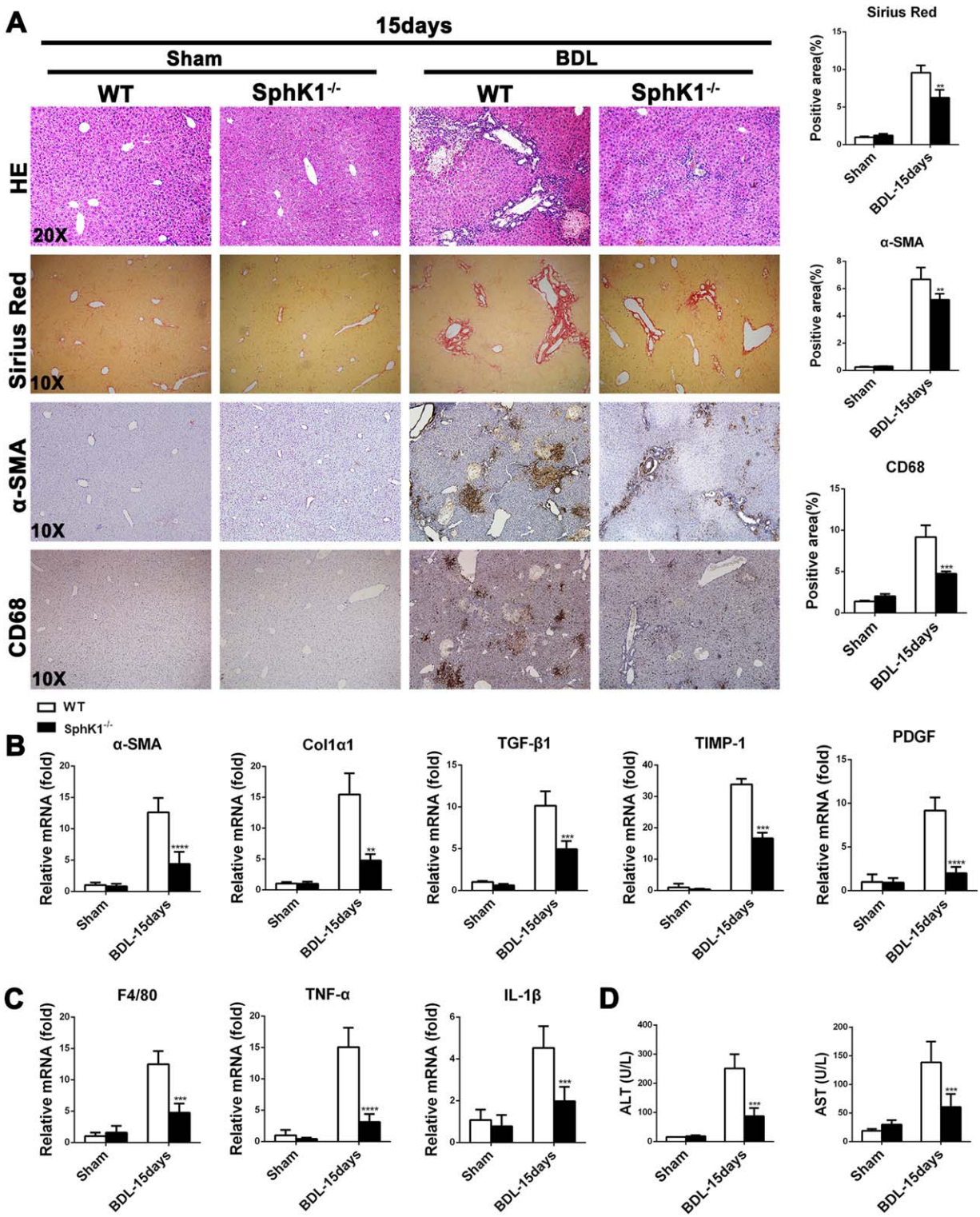


**FIG. 3.** SphK1 contributes to BDL-induced liver fibrosis in mice. WT and SphK1$^{-/-}$ mice were operated by BDL for 15 days. (A) Representative histology of H&E, Sirius Red and IHC staining of α-SMA and CD68 in the liver of mice operated with sham or BDL. Quantification of positive staining areas were measured by Image J software. Hepatic mRNAs of fibrogenic genes (B) and inflammatory genes (C) were measured by qRT-PCR assays in WT and SphK1$^{-/-}$ mice induced by BDL. (D) Serum levels of ALT and AST. $^{**}P<0.01$; $^{***}P<0.001$; $^{****}P<0.0001$ versus WT mice operated with BDL or sham.

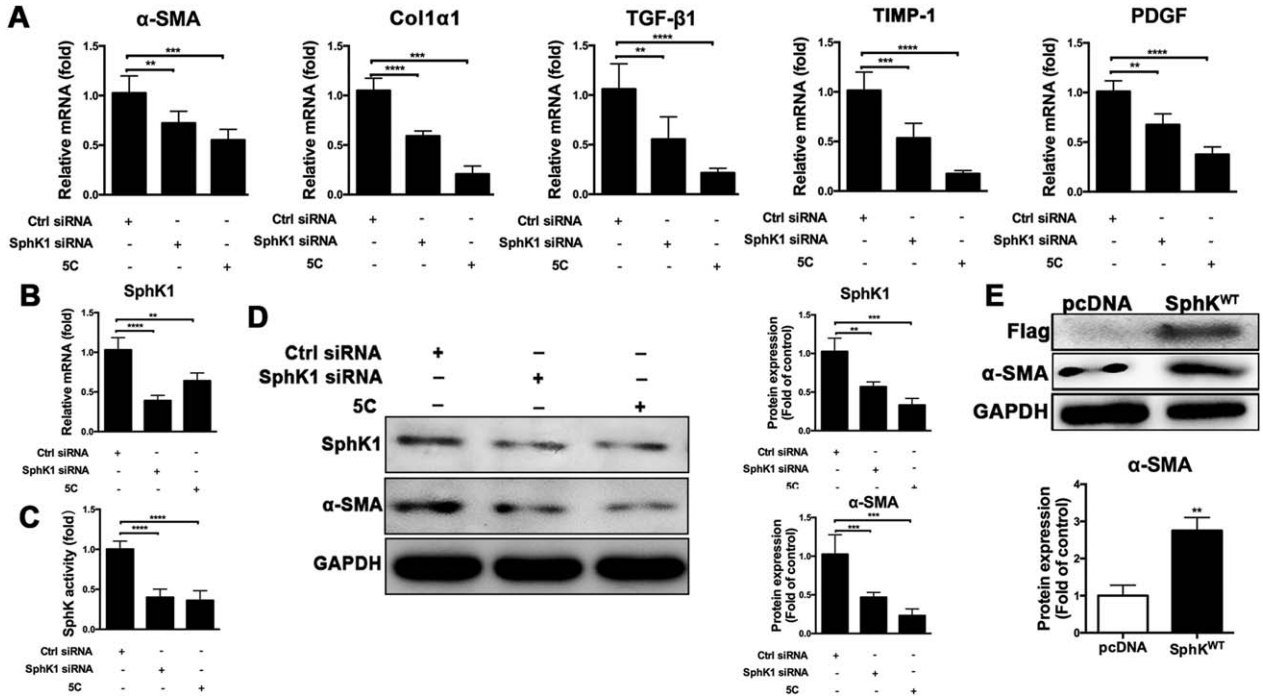


**FIG. 4.** SphK1 upregulates α-SMA and fibrogenic genes in activated HSCs (LX-2 cells). (A) LX-2 cells were transfected with SphK1 siRNA for 48 hours or treated with SphK1 specific inhibitor 5C (100 nM) for 24 hours. Hepatic mRNAs of fibrogenic genes were measured by qRT-PCR assays. (B) Quantitative PCR analyses of SphK1 from LX-2 cells transfected with SphK1 siRNA for 48 hours or treated with 5C for 24 hours. (C) SphK1 activity was measured by LC–MS/MS. (D) Immunoblotting assays of SphK1 and α-SMA in LX-2 cells transfected with SphK1 siRNA for 48 hours or treated with 5C for 24 hours. Quantification of bands for SphK1 and α-SMA were measured by Image J software. (E) LX-2 cells were transfected with SphK1 plasmid or pcDNA (vector) for 48 hours. Representative immunoblotting bands of Flag and α-SMA and quantitated by Image J software. $^{**}P<0.01$; $^{***}P<0.001$; $^{****}P<0.0001$ versus Control.

## SphK1 DEFICIENCY MAINLY ATTENUATES CHEMOKINE CCL2 SECRETION IN FIBROTIC MOUSE LIVER AND KCS

Inflammatory chemokines known to be critical for the pathogenesis of liver fibrosis. To determine the change of chemokine expression in liver fibrosis, liver tissue lysates from control or fibrotic mice induced by $CCl_4$ were examined using the chemokine array that contains 25 different chemokine antibodies. We found three chemokines (CCL1, CCL2 and CXCL12) were increased in WT mice, while they were decreased in SphK1$^{-/-}$ mice. Especially, CCL2 is one of the most elevated chemokines and dramatically downregulated by SphK1 deficiency (Fig. 5A). Repression of CCL2 gene expression by SphK1 deficiency was further verified by the results of qRT-PCR assays in mice induced by $CCl_4$ or BDL (Fig. 5B). Liver injury triggers KC activation, leading to inflammatory cytokine and chemokine release.[27] Next, we determined the role of SphK1 in CCL2 secretion in KCs. qRT-PCR assay shown that the CCL2 mRNA was significantly reduced in SphK1-deficient KCs compared with WT KCs (Fig. 5C), suggesting that SphK1 is required for CCL2 production in KCs.

## SphK1 MEDIATES CCR2 UPREGULATION AND ACTIVATION IN HSCS INDUCED BY CCL2

CCL2 was found to promote migration and positioning of HSCs.[28] In addition, CCR2 promotes HSC chemotaxis and the development of hepatic fibrosis.[11] To define the effects of SphK1 on the CCL2-CCR2 signaling in HSCs, we performed immunofluorescence double staining of CCL2 with α-SMA (activated HSC marker). In the oil control mice, we found very weak expression of CCR2. However, CCR2 was dramatically augmented in α-SMA$^+$HSCs (Fig. 5D), suggesting that SphK1 regulates CCR2 expression in HSCs. Given that CCL2 acts

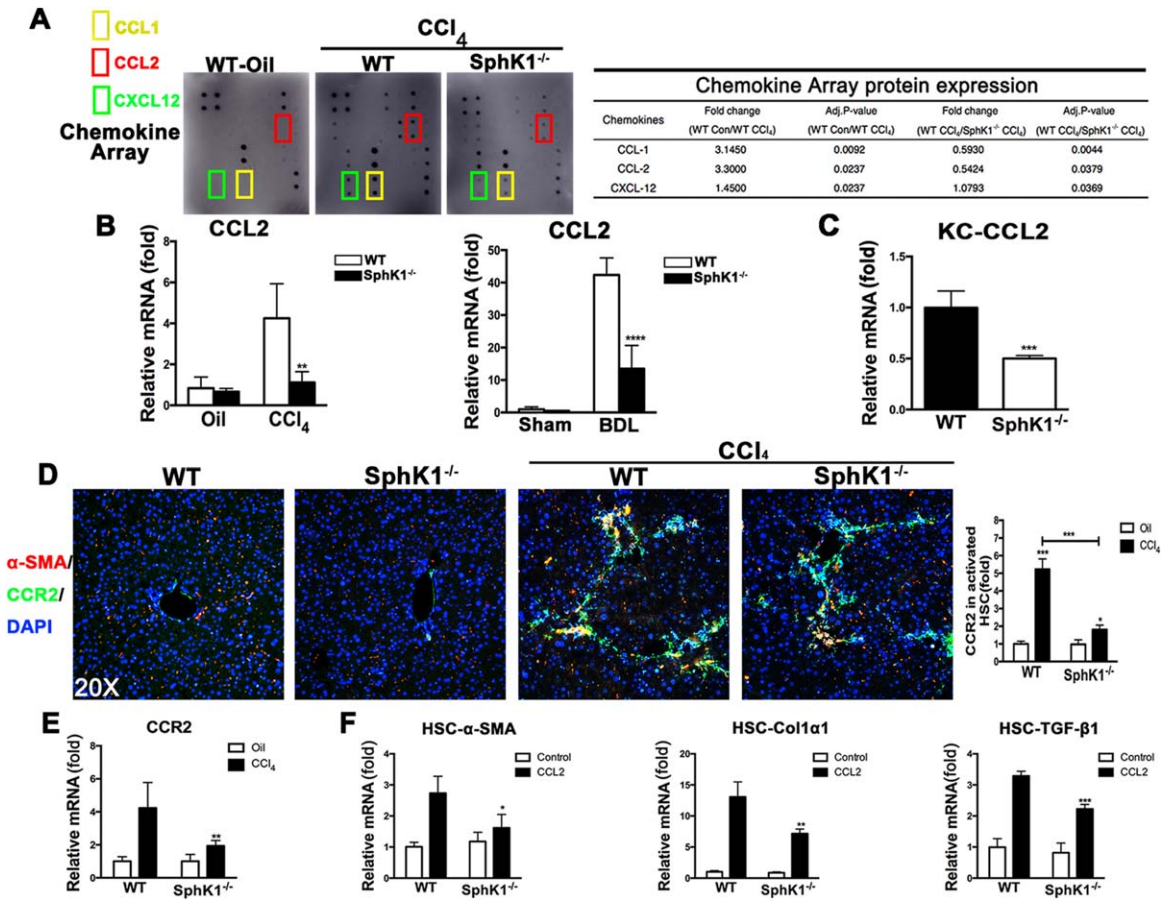


**FIG. 5.** The chemokine (CCL2–CCR2) signaling axis induces liver fibrosis via SphK1 activation. (A) The left panel is a schematic representation of the antibody-based protein array containing 25 chemokines with duplicates. The array contains two positive controls (PC) and one negative control (NC). The expression level of chemokines in liver lysates from the WT and SphK1$^{-/-}$ mice induced by $CCl_4$ is shown. The CCL1 (in yellow), CCL2 (in red) and CXCL12 (in green) were upregulated in $CCl_4$-treated WT mice compared with oil control, whereas downregulated in $CCl_4$-treated SphK1$^{-/-}$ mice. The fold changes of CCL1, CCL2 and CXCL12 were shown in the right panel. (B) qRT-PCR analyses of hepatic CCL2 mRNA from WT and SphK1$^{-/-}$ mice induced by $CCl_4$ for 6 weeks or BDL for 15 days. (C) qRT-PCR analyses of CCL2 in KCs from WT and SphK1$^{-/-}$ mice. (D) Representative immunostaining images shown that the expression of CCR2 colocalized with activated HSCs marker, α-SMA in liver from WT and SphK1$^{-/-}$ mice induced by $CCl_4$ for 6 weeks. DAPI staining was used to identify the nuclei. Summarized histogram shows the average area of co-localization of CCL2 with α-SMA per field. (E) qRT-PCR analyses for CCR2 mRNA in liver from WT and SphK1$^{-/-}$ mice induced by $CCl_4$ for 6 weeks. (F) Primary HSCs were isolated from WT and SphK1$^{-/-}$ mice and cultured for 1 day, and then treated with CCL2 (50 ng/mL) for 24 hours. qRT-PCR analyses for fibrogenic genes mRNA in primary HSCs. *$P$<0.05; **$P$<0.01; ***$P$<0.001; ****$P$<0.0001 versus Control. Abbreviations: NC, negative control; PC, positive control.

through its receptor CCR2 in mediating HSC activation,[11,28] we next examined the role of SphK1 in the activation of HSC induced by CCL2. The expression of CCR2 in primary HSCs isolated from WT mouse liver was significantly induced by CCL2. However, CCR2 was dramatically reduced in SphK1-deficient HSCs (Fig. 5E). Additionally, qRT-PCR assays for fibrogenic factors (α-SMA, Col1α1 and TGF-β1) verified the inhibitory effect of HSC-specific deletion of SphK1 on fibrogenic gene induction by CCL2 (Fig. 5F).

## MiR-19b-3p, DIRECTLY BINDING TO 3′-UTR REGION OF CCR2 mRNA, IS REPRESSED BY $CCl_4$-INDUCED LIVER FIBROSIS AND RESTORED BY SphK1 DEPLETION

To investigate the differences in miRNA expression profiles between fibrotic and normal livers, we performed miRNA microarrays for total RNA extracts isolated from mouse livers treated with $CCl_4$ or corn

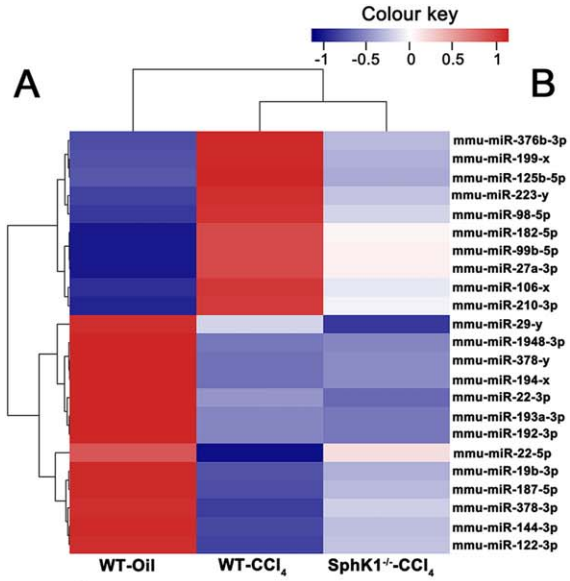


| Downregulated miRNAs | | |
|---|---|---|
| miRNA | Fold change (WT $CCl_4$/WT Con) | Fold change (SphK1$^{-/-}$ $CCl_4$/WT $CCl_4$) |
| miR-19b-3p | 0.19306 | 1.93424 |
| miR-187-5p | 0.55888 | 1.19712 |
| miR-22-5p | 0.60968 | 1.40895 |
| miR-1948-3p | 0.21154 | 1.13275 |
| miR-193a-3p | 0.48156 | 0.96648 |
| miR-192-3p | 0.47577 | 0.94703 |
| miR-29-y | 0.69024 | 0.76296 |
| miR-144-3p | 0.56111 | 1.21886 |
| miR-378-y | 0.78079 | 1.01715 |
| mR-194-x | 0.68973 | 1.02874 |
| miR-22-3p | 0.74414 | 0.95316 |
| miR-378-3p | 0.80639 | 1.08056 |
| miR-122-3p | 0.49943 | 1.29661 |
| Upregulated miRNAs | | |
| miRNA | Fold change (WT $CCl_4$/WT Con) | Fold change (SphK1$^{-/-}$ $CCl_4$/WT $CCl_4$) |
| miR-376b-3p | 1.61952 | 0.71281 |
| miR-199-x | 3.27509 | 0.45533 |
| miR-106-x | 1.60834 | 0.77995 |
| miR-210-3p | 2.95110 | 0.64314 |
| miR-182-5p | 1.95750 | 0.77919 |
| miR-223-y | 2.85789 | 0.54213 |
| miR-99b-5p | 3.04368 | 0.70556 |
| miR-98-5p | 1.41587 | 0.80836 |
| miR-27a-3p | 2.35729 | 0.74713 |
| miR-125b-5p | 2.23353 | 0.56103 |

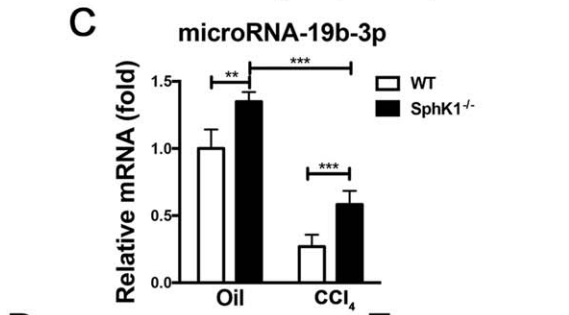


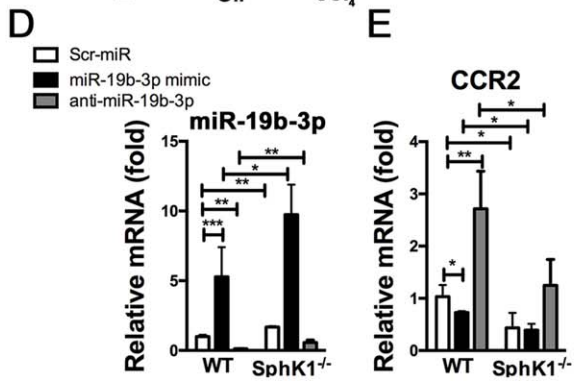


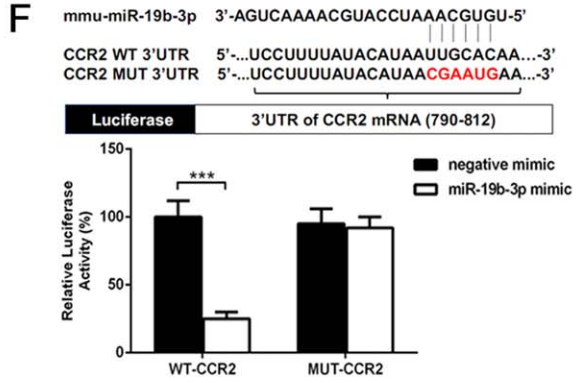


**FIG. 6.** SphK1 mediates the activation of HSCs and $CCl_4$-induced liver fibrosis in mice via downregulation of miR-19b-3p. (A) Microarray analysis for miRNA expression was performed with total RNA extracted from livers of mice treated with corn oil (WT-oil) or $CCl_4$ for 6 weeks. Heat map shows the two-way hierarchical clustering of differentially expressed miRNAs. Each row and column represents an miRNA and a condition, respectively. The row Z-score scaling for the expression level of each miRNA was calculated by subtracting the mean expression of the miRNA from its expression value and then dividing by the SD across all the samples. The closer the color is to bright blue, the lower the expression; the closer to bright red, the higher the expression. (B) A list of significantly dysregulated miRNAs in $CCl_4$-treated compared with corn-oil-treated livers is shown with the fold change. (C) qRT–PCR was performed to assess expression of the miR-19b-3p in livers from the oil or $CCl_4$-treated WT mice, as well as $CCl_4$-treated SphK1$^{-/-}$ mice at 6 weeks (n = 8 per group). (D-E) Primary aHSCs were transfected with a scrambled (Scr)-miR (control, white bar), mimic miR-19b-3p (black bar) or anti-miR-19b-3p (gray bar) oligonucleotide for 48 hours, and mRNA levels of miR-19p-3p (D) andCCR2 (E) were analyzed by qRT–PCR assays. (F) Dual-luciferase reporter assays were performed to test the interaction of mmu miR-19b-3p and its targeting sequence in the CCR2 mRNA 3′-UTR using GP-miRGLO plasmid constructs containing the predicted targeting sequence (WT-CCR2) and mutated targeting sequence (MUT-CCR2) cloned into the 3′-UTR of the reporter gene. The mutated nucleotides were underlined. Plasmids were transfected into primary HSCs together with miR-19b-3p mimic or negative mimic control. The luciferase activity was determined after 48 hours of transfection. Data represent three independent experiments with triplicate measurements. Data are presented as means ± SD $^{*}P<0.05$; $^{**}P<0.01$; $^{***}P<0.001$ versus Control.

oil for 6 weeks (n = 6 per group). The miRNAs were considered to have significant differences in expression level when the expression difference showed more than two-fold change between the experimental and control groups at $P < 0.05$. We found that the expression of 23 miRNAs were altered in fibrotic liver. Thirteen miRNAs were downregulated and the other 10 were upregulated in the $CCl_4$ group compared with the control. Among these miRNAs downregulated in liver fibrosis, miR-19b-3p had the lowest expression in the livers of $CCl_4$-treated WT mice (0.193-fold). This reduced expression of miR-19b-3p was restored in $CCl_4$-treated SphK1$^{-/-}$ mice (1.934-fold) (Fig. 6A,B). qRT-PCR assays for miR-19b-3p verified that SphK1 depletion restored the repression of miR-19b-3p by $CCl_4$-induced liver fibrosis (Fig. 6C). To confirm these findings *in vivo*, we isolated primary HSCs from WT and SphK1$^{-/-}$ mice. As primary HSCs are known to be activated during culture, we found that miR-19b-3p was significantly downregulated at day 5 (activated HSCs) compared with day 0 (quiescent HSCs) of culture (Fig. 6D), these results indicate that these miRNAs were downregulated during HSC activation. Next, primary HSCs were transfected with miR-19b-3p mimic or anti-miR-19b-3p and cultured for 5 days. As expected, miR-19b-3p mRNA was significantly increased in miR-19b-3p mimic-transfected cells, whereas decreased in anti-miR-19b-3p-transfected cells (Fig. 6D). To identify the relevant target genes of the miR-19b-3p, we conducted bioinformatics analysis using http://www.targetscan.org/, a comprehensive resource of miRNA target predictions. We found that CCR2 was a potential target of miR-19b-3p in mice (Supporting Fig. S3A). We next investigated whether ectopic expression of miR-19b-3p in the aHSCs influenced CCR2 expression and HSC activation. As expected, mRNA levels of CCR2 was significantly downregulated in miR-19b-3p-mimic-transfected WT cells, whereas upregulated in anti-miR-19b-3p-transfected WT cells. In contrast, CCR2 upregulation by anti-miR-19b-3p was reversed by SphK1 depletion in HSCs (Fig. 6E). Furthermore, we investigated whether miR-19b-3p interacted with the binding sites at the 3′-untranslated region (3′-UTR) of CCR2 mRNA using luciferase assay in primary HSCs. We cloned a 3′-UTR fragment of CCR2 into pGL3 luciferase reporter vector. These segments included a predicted binding site for miR-19b-3p (Fig. 6F). Overexpression of miR-19b-3p in HSCs markedly decreased the luciferase activity of 3′-UTR in the WT reporter of CCR2. However, the activity was not significantly changed in HSCs transfected with mutant reporter plasmid of CCR2. In addition, there was no effect on the 3′-UTR activity following treatment with the miR-negative control (Fig. 6F). Together, our luciferase reporter assay confirmed that miR-19b-3p directly bound to CCR2 mRNA. Consistently, in primary aHSCs transfected with a miR-19b-3p mimic, expression of the fibrogenic genes encoding for α-SMA, Col1α1 and TIMP-1 was decreased, whereas further increased in aHSCs transfected with anti-miR-19b-3p. Interestingly, the upregulation of fibrogenic genes in aHSCs by anti-miR-19b-3p transfection was significantly reversed by SphK1 depletion (Supporting Fig. S3B-E). Therefore, these results demonstrate that SphK1 deficiency induces miR-19b-3p upregulation, and subsequently attenuates the activation of HSCs by targeting CCR2.

## SphK1 ON RESIDENT CELLS, BUT NOT BM-DERIVED CELLS, ARE CRITICAL FOR LIVER FIBROSIS

Because SphK1 is important for liver fibrosis of two animal models and is expressed both in HSCs and KCs (Fig. 7A, Supporting Fig. S1), we investigated which cell types are critical in SphK1-mediated liver fibrosis. We generated SphK1-chimeric mice by using a combination of KC depletion (Supporting Fig. S4), irradiation, and BMT. Liposomal clodronate was injected intraperitoneally to deplete resident KCs after 2 weeks of BMT (Supporting Fig. S4). This combination generates complete substitution of KCs and other BM-derived cells, but not of resident hepatic cell populations, including HSCs. Because SphK1 is not expressed in hepatocytes, this protocol reconstitutes KCs, but not HSCs, with BM-derived cells. Thus, we generated two types of SphK1-chimeric mice:

1. WT mice with transplanted SphK1$^{-/-}$ BM, which contained SphK1$^{-/-}$ KCs and WT HSCs
2. SphK1$^{-/-}$ mice with transplanted with WT BM, which contained WT KCs and SphK1$^{-/-}$ HSCs.

After a two-month recovery, hepatic fibrosis was induced by way of $CCl_4$ treatment. After 6 weeks of induction, WT mice transplanted with WT BM (WT BM→WT) had significantly increased collagen deposition as assessed by Sirius red staining. However, SphK1 chimeric mice with SphK1-deficient endogenous liver cells (WT BM→SphK1$^{-/-}$ and SphK1$^{-/-}$ BM→SphK1$^{-/-}$) had reduced fibrosis compared with WT BM→WT mice (Fig. 7A). In agreement with the

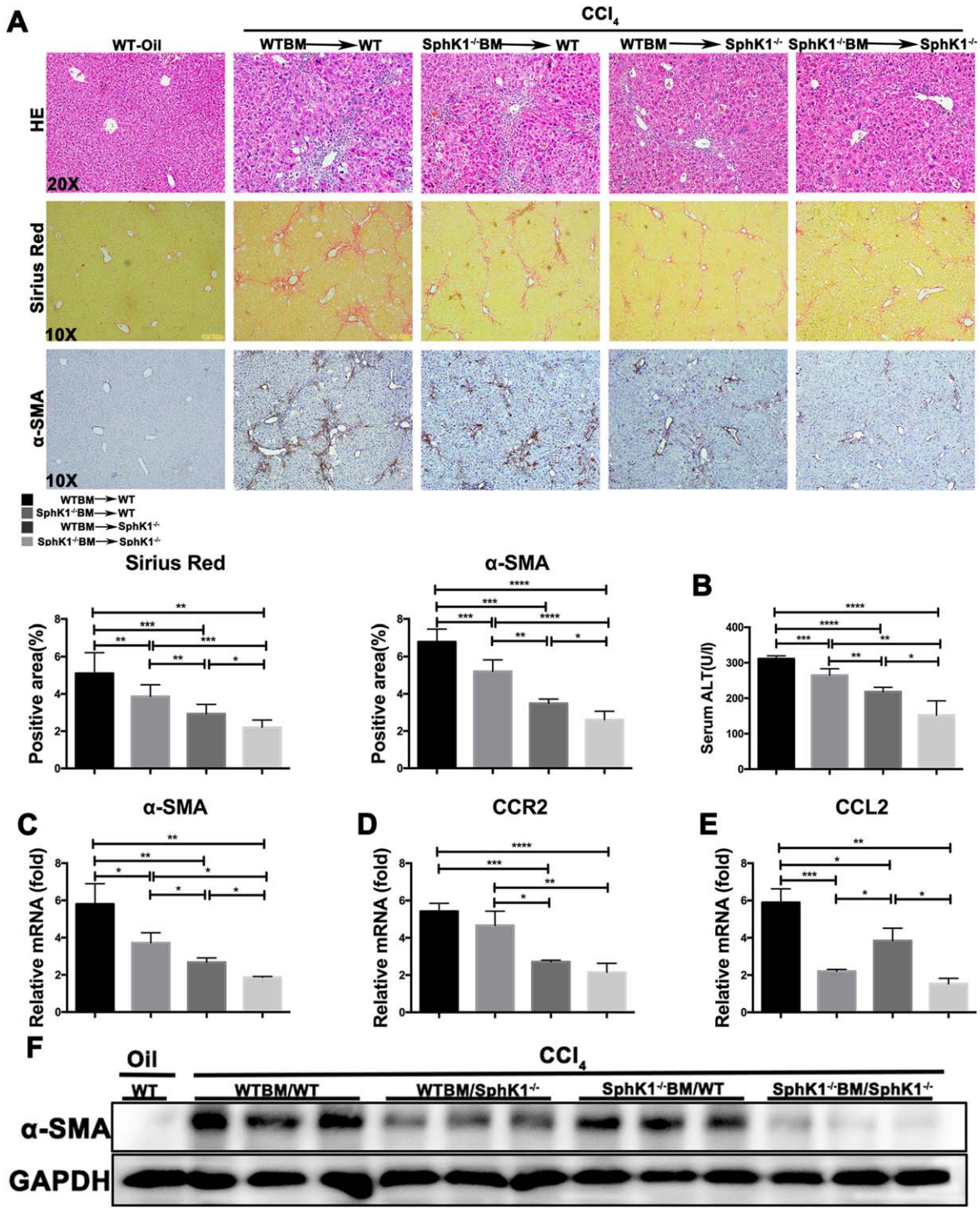


**FIG. 7.** Chimeric mice with SphK1-deficient endogenous liver cells show decreased hepatic fibrosis after $CCl_4$ induction. Chimeric mice were generated by transplanting WT or SphK1$^{-/-}$ BM into irradiated and clodronate-treated WT mice or SphK1$^{-/-}$ mice. Liver fibrosis was induced by 12 injections of $CCl_4$ (1 ml/kg; intraperitoneal injection) for 6 weeks. (A) Representative histology of H&E, Sirius Red and α-SMA IHC staining are shown. Quantification of positive staining areas were measured by Image J software. (B) Liver injury was measured by serum levels of ALT. (C-E) Hepatic mRNA levels of α-SMA (C), CCR2 (D) and CCL2 (E) were analyzed by qRT-PCR. (F) Hepatic expression of α-SMA in chimeric mice was measured by immunoblotting assay. $^{*}P<0.05$; $^{**}P<0.01$; $^{***}P<0.001$; $^{****}P<0.0001$ versus transplanting WT BM into irradiated and clodronate-treated WT mice with $CCl_4$.

results on collagen deposition, WT BM→WT mice showed an increased expression of α-SMA comparable to WT-oil mice, whereas SphK1$^{-/-}$ mice containing WT BM (WT BM→SphK1$^{-/-}$) had decreased α-SMA expression similar to SphK1$^{-/-}$ mice transplanted with SphK1$^{-/-}$ BM (SphK1$^{-/-}$ BM→SphK1$^{-/-}$) (Fig. 7A,C,F). As expected, serum levels of ALT were lower in SphK1 chimeric mice with SphK1-deficient endogenous liver cells (WT BM→SphK1$^{-/-}$ and SphK1$^{-/-}$ BM→SphK1$^{-/-}$) compared with WT mice transplanted with WT BM (WT BM→WT) (Fig. 7B). However, SphK1 chimeric mice that expressed SphK1 in endogenous liver cells but not BM-derived cells (SphK1$^{-/-}$ BM→WT) had a lesser reduced liver fibrosis compared with SphK1 chimeric mice with SphK1-deficient endogenous liver cells (WT BM→SphK1$^{-/-}$ and SphK1$^{-/-}$ BM→SphK1$^{-/-}$) (Fig. 7A–C,F). On the contrary, SphK1$^{-/-}$ chimeric mice that express SphK1 in BM-derived cells but not endogenous liver cells (WT BM→SphK1$^{-/-}$) showed the similar reduction of liver fibrosis as mice with complete depletion of SphK1$^{-/-}$ (SphK1$^{-/-}$ BM→SphK1$^{-/-}$) (Fig. 7D). However, WT or SphK1$^{-/-}$ mice transplanted with SphK1$^{-/-}$ BM showed decreased secretion of CCL2 compared with WT or SphK1$^{-/-}$ mice transplanted with WT BM (Fig. 7E). Taken together, these results suggest that SphK1 expression on recipient-originated cells including HSCs is required for the pathogenesis of liver fibrosis, whereas SphK1 has a lesser role in liver fibrosis in BM-derived cells including macrohage.

## INHIBITING SphK1 SIGNALING ALLEVIATES MURINE LIVER FIBROSIS

On the basis of SphK1 deficiency significantly attenuating development of liver fibrosis in mice subjected to $CCl_4$ or BDL, we finally examined the effect of SphK1 specific inhibitor (5C) on the potential treatment of liver fibrosis in mice induced by $CCl_4$ or BDL. H&E and Sirius red staining assays revealed that 5C treatment alleviates $CCl_4$-induced as compared with vehicle controls. Accordingly, 5C notably reduced α-SMA-staining intensities in the fibrotic livers (Fig. 8A). The qRT-PCR assay showed that 5C also significantly reduced the mRNA levels of fibrogenic genes (α-SMA, Col1α1, TGF-β1, TIMP-1 and PDGF) (Fig. 8B). Similarly, an immunoblotting assay verified that repression of α-SMA expression by 5C treatment (Fig. 8C). In serum biochemistry analyses, ALT was significantly diminished by 5C treatment, indicative of improvement of liver function (Fig. 8D). Similar results were obtained in BDL-induced liver fibrosis in mice treated with 5C (Supporting Fig. S6), suggesting that blockage of SphK1 signaling significantly ameliorates the pathogenesis of liver fibrosis of different etiologies in mice.

# Discussion

Earlier studies have demonstrated the relevance of SphK1 signaling activation in chronic liver injury and fibrosis.[20,24-26] However, the *in vivo* role of SphK1 deficiency in the pathogenesis of liver fibrosis has been unclear. In the current study, we first used SphK1$^{-/-}$ mice to verify that genetic or pharmacological inactivation of SphK1 attenuated acute and chronic liver injury and fibrosis in mice.

We showed that knockout of SphK1 in mice diminished liver fibrosis with recovery of liver function in $CCl_4$- or BDL-induced animal models of liver fibrosis, indicating that deficiency of SphK1 could effectively attenuate the progression of liver fibrosis. In addition, SphK1 knockout prevented the early fibrogenic events initiated by acute liver injury. Consistently, SphK1 specific inhibitor 5C diminished chronic liver injury and fibrosis induced by $CCl_4$. Previous studies also showed that SphK inhibitor DMS or SKI attenuated collagen deposition and angiogenesis to protect against liver fibrosis,[24,25] although DMS or SKI was not specific to SphK1. All of these findings support the conclusion that attenuation of SphK1 signaling prohibits the development and progression of liver fibrosis.

One of the tasks to thoroughly understand the role of SphK1 for liver fibrosis is to characterize and identify their cell-type-specific functions under different conditions. Parenchymal and nonparenchymal liver cells as well as immune infiltrating cells contribute to mechanism of liver injury and fibrosis. Thus, cell-type-specific activation of SphK1 might be relevant to determine the outcome of liver disease. In the present study, our interest focused on defining the relevance of SphK1 activation in different liver cell compartments during liver fibrosis. Investigation of SphK1 expression in the liver of patients with fibrosis or different experimental murine models revealed that the SphK1 expression was upregulated in the fibrotic liver, and positively correlated with the disease progression; this event was particularly associated with the activation of HSCs.

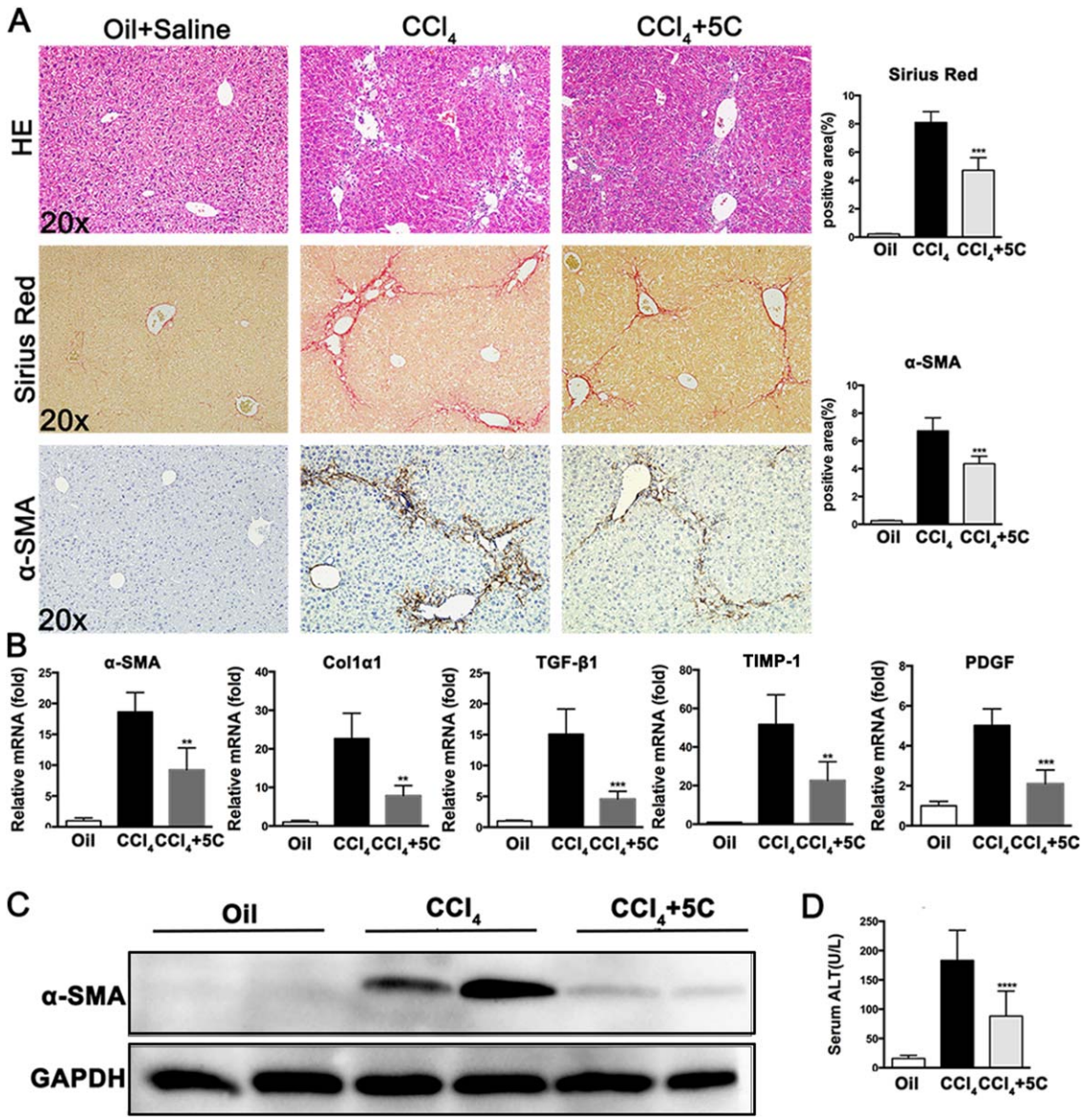


**FIG. 8.** SphK1 inhibitor reverses $CCl_4$-induced liver fibrosis in mice. B6 mice were administered with $CCl_4$ (1 ml/kg; intraperitoneal injection) twice per week for 6 weeks, in combination with intraperitoneal injections of SphK1 specific inhibitor (5C, 10 mg/kg) and saline control twice per week for 6 weeks. (A) Representative images of H&E, Sirius Red and α-SMA IHC staining of liver sections. Quantification of positive areas of histological images were measured by Image J software. (B) Hepatic mRNAs of fibrogenic genes were measured by qRT-PCR assays in B6 mice treated with 5C or vehicle after $CCl_4$ induction. (C) Immunoblotting analyses of α-SMA expression in the mouse liver tissues. (D) Liver function was assessed by serum levels of ALT in mice. $^{**}P<0.01$; $^{***}P<0.001$; $^{****}P<0.0001$ versus B6 mice treated with $CCl_4$.

Immunohistochemistry assay showed that SphK1 mainly expressed in non-parenchymal area rather than parenchymal area (hepatocytes) both in human and rodent livers. Furthermore, immuohistofluorescence revealed that both KCs and HSCs expressed SphK1 in normal and fibrotic livers. The recruitment and migration of KCs and HSCs are critical events for developing liver injury and fibrosis. Additionally, most extracellular matrix components are produced by HSCs, and accumulation of these ECM causes liver fibrosis. Cytokines and chemokines stimulate key biological processes in HSCs, such as activation, proliferation, and migration.[29] Moreover, KCs can interact with HSCs, accelerate their activation and promote

their fibrogenic response *in vitro*.[30] Previous studies reported that BMSCs in damaged liver induced by $CCl_4$. Furthermore, TGF-$\beta$1 induced BMSC differentiation to myofibroblasts accompanied by the upregulation of SphK1.[26]

To identify the most relevant target cell of SphK1-mediated profibrotic effects, WT or SphK1$^{-/-}$ mice were reconstituted with BM from WT or SphK1$^{-/-}$ donors. Our results showed that SphK1 in HSCs majorly contribute to liver fibrosis than SphK1 in KCs. Additionally, increased SphK1 was confirmed in both human HSC LX-2 cells and primary mouse HSCs, and inhibition of SphK1 signaling abrogated HSC activation. These data suggested that SphK1 in HSCs play the major roles in the progression of liver injury and fibrosis.

As firmly established in the literature, disruption of CCR2 signaling impedes liver fibrosis as evidenced by altered the chemotaxis and transdifferentiation of HSCs.[11] Recruitment of immune cells such as KCs and HSCs to the site of injury and inflammation is an important event in regeneration, wound healing, and hepatic fibrosis.[31] Chemokines and chemokine receptors have a central role in the regulation of cell migration and local inflammation.[32] The CCR2 ligand CCL2 can be produced by KCs, which promotes liver fibrosis by recruitment of macrophages that are associated with HSCs.[3,33] In human liver diseases, increased CCL2 is associated with macrophage recruitment and liver fibrosis progression.[13] In addition, the inactivation of CCL2 attenuates $CCl_4$-induced liver injury and fibrosis by inhibiting macrophage recruitment.[33] An important finding of our current study is identification of the paracrine effect of SphK1-mediated CCL2 secretion produced by KC on HSC activation (Fig. 5). Furthermore, KCs co-culture promoted HSC migration (Supporting Fig. S5). Our present study also demonstrated that SphK1 on KCs is required for the secretion of CCL2, however, SphK1 on KCs is not very dispensable for the HSC activation and collagen deposition. Notably, SphK1 on recipient-originated cells including HSCs is more important than SphK1 on KCs in the regulation of HSC activation and rodent fibrogenesis induced by $CCl_4$. Our current study found a regulatory effect of SphK1 on CCL2-CCR2 axis in KCs and HSCs and subsequent promotion of liver fibrogenesis. Moreover, our *in vitro* results confirmed the *in vivo* findings and demonstrated that SphK1 is crucial for HSC activation and ECM deposition. Deficiency of SphK1 reduced migration and activation of HSCs associated with downregulation of CCR2 and downstream fibrotic genes.

Recent miRNA microarray analysis performed on quiescent and activated HSCs showed that miR-19b was dramatically downregulated in activated HSCs. Similarly, miR-19b expression was markedly downregulated in fibrotic human livers. miR-19b mimic negatively regulated TGF-$\beta$ signaling components demonstrated by decreased its direct target gene, TGF-$\beta$ receptor 2 (TGF-$\beta$R2), preventing activated HSC phenotype and progression of rodent liver fibrosis.[34] We analyzed liver tissues of mice treated with $CCl_4$ for 6 weeks unique mouse miRNA Microarray. Consistently, our results demonstrated that expression of miR-19b-3p declined in fibrotic livers of mouse models with hepatic injury and also in activated HSCs. In addition, miR-19b-3p mimic also downregulated TGF-$\beta$R2 in activated HSCs (Supporting Fig. S3D). In particular, we found evidence that expression of miR-19b-3p was downregulated by SphK1, and reduced miR-19b-3p directly upregulated CCR2 by binding the 3′-UTR region of CCR2 mRNA in mouse, which is vital for efficient activation of downstream profibrotic genes, contributing to the pathogenesis of liver fibrosis.

Another important finding of our study is discovery of the presence of miR-19b-3p in HSCs and the inhibitory role of miR-19b-3p in CCR2-mediated liver fibrosis. Hepatic level of miR-19b-3p was decreased in $CCl_4$-treated WT mice, whereas increased in $CCl_4$-treated SphK1$^{-/-}$ mice. In addition, miR-19b-3p expression was raised in SphK1-deficient HSCs compared with WT HSCs. Moreover, either SphK1 deficiency or exogenous miR-19b-3p mimic abrogated the expression of CCR2 and fibrogenic factors. Additionally, expression of fibrogenic genes was markedly induced by anti-miR-19b-3p even in activated HSCs deficient with SphK1. These data suggested that SphK1 deficiency downregulate CCR2 via upregulation of miR-19b-3p in HSCs as well as fibrotic liver.

Recent studies reported that manipulating the expression of dysregulated miRNAs showed an antifibrotic effect in mouse model of $CCl_4$-induced liver fibrosis.[35,36] Our current study also demonstrated that upregulation of miR-19b-3p by SphK1 deficiency attenuated $CCl_4$-induced liver fibrosis. However, the systemic delivery of RNA-based therapeutics *in vivo* remains a challenge due to the presence of serum nucleases in blood, the poor uptake by the cells in the targeted tissues and rapid clearance by the renal

system.[37] The newly-developed nanomedicine can minimize these negative effects. Recently, nanoparticles (NPs) made from an amino acid-based polymer have been shown to effectively transfect tissue *in vivo*. Rodent liver fibrosis was rescued by even a single injection of NPs having miR-378a-3p.[38] Thus, miR-19b-3p encapsulated with NPs will need to be developed as RNA delivery vehicles to validate the therapeutic roles of miR-19b-3p in the treatment of liver fibrosis.

In conclusion, our current study demonstrates that SphK1 has distinct roles in KCs and HSCs in the pathogenesis of liver injury and fibrosis. SphK1 on KCs regulates the migration of KCs and secretion of CCL2. Furthermore, SphK1 expressed in HSCs is more crucial for the pathogenesis of liver fibrosis. Our study also demonstrates that miR-19b-3p suppresses the activation of HSCs by targeting CCR2, and SphK1-deficient HSCs repress the transcriptional expression of miR-19b-3p to suppress the expression of CCR2 and the activation of HSCs, protecting against liver fibrosis. The interaction of SphK1-CCL2-CCR2 as a key molecular event in the activation of HSCs. All of these results strengthen the conclusion that activation of SphK1 signaling in HSCs and KCs indeed contributes to the development and progression of liver fibrosis (Supporting Fig. S7). These findings indicate that SphK1 has great potential to be used as a therapeutic agent for treating liver fibrosis.

*Acknowledgment:* We thank Dr. Pu Xia from Fudan University, China; Dr. Ke Shuai from UCLA, and Dr. Wai Wilson Cheung from UCSD for their instruction and assistance. We are grateful to Guangzhou Biocytocare Biotechnology Co.,Ltd. for assistance with primary liver cell isolation. We thank Rui Li, Sishan Yan, Yishan Li, Cuiyun Li, Jiayi Liu, and Wanlan Yu from Guangdong Pharmaceutical University for their assistance throughout the study.

## REFERENCES

1) Friedman SL. Mechanisms of hepatic fibrogenesis. Gastroenterology 2008;134:1655-1669.
2) Schuppan D, Ruehl M, Somasundaram R, Hahn EG. Matrix as a modulator of hepatic fibrogenesis. Semin Liver Dis 2001;21: 351-372.
3) Seki E, De Minicis S, Osterreicher CH, Kluwe J, Osawa Y, Brenner DA, Schwabe RF. TLR4 enhances TGF-beta signaling and hepatic fibrosis. Nat Med 2007;13:1324-1332.
4) Novo E, Cannito S, Paternostro C, Bocca C, Miglietta A, Parola M. Cellular and molecular mechanisms in liver fibrogenesis. Arch Biochem Biophys 2014;548:20-37.
5) Wynn TA. Cellular and molecular mechanisms of fibrosis. J Pathol 2008;214:199-210.
6) **Mederacke I**, **Hsu CC**, **Troeger JS**, Huebener P, Mu X, Dapito DH, Pradere JP, et al. Fate tracing reveals hepatic stellate cells as dominant contributors to liver fibrosis independent of its aetiology. Nat Commun 2013;4:2823.
7) **Pradere JP**, **Kluwe J**, De Minicis S, Jiao JJ, Gwak GY, Dapito DH, et al. Hepatic macrophages but not dendritic cells contribute to liver fibrosis by promoting the survival of activated hepatic stellate cells in mice. HEPATOLOGY 2013;58:1461-1473.
8) Duffield JS, Forbes SJ, Constandinou CM, Clay S, Partolina M, Vuthoori S, et al. Selective depletion of macrophages reveals distinct, opposing roles during liver injury and repair. J Clin Invest 2005;115:56-65.
9) Karlmark KR, Weiskirchen R, Zimmermann HW, Gassler N, Ginhoux F, Weber C, et al. Hepatic recruitment of the inflammatory Gr1+ monocyte subset upon liver injury promotes hepatic fibrosis. HEPATOLOGY 2009;50:261-274.
10) Zimmermann HW, Seidler S, Nattermann J, Gassler N, Hellerbrand C, Zernecke A, et al. Functional contribution of elevated circulating and hepatic non-classical CD14CD16 monocytes to inflammation and human liver fibrosis. PLoS One 2010; 5:e11049.
11) Seki E, de Minicis S, Inokuchi S, Taura K, Miyai K, van Rooijen N, et al. CCR2 promotes hepatic fibrosis in mice. HEPATOLOGY 2009;50:185-197.
12) Mitchell C, Couton D, Couty JP, Anson M, Crain AM, Bizet V, et al. Dual role of CCR2 in the constitution and the resolution of liver fibrosis in mice. Am J Pathol 2009;174:1766-1775.
13) Marra F, DeFranco R, Grappone C, Milani S, Pastacaldi S, Pinzani M, et al. Increased expression of monocyte chemotactic protein-1 during active hepatic fibrogenesis: correlation with monocyte infiltration. Am J Pathol 1998;152:423-430.
14) Baeck C, Wehr A, Karlmark KR, Heymann F, Vucur M, Gassler N, Huss S, et al. Pharmacological inhibition of the chemokine CCL2 (MCP-1) diminishes liver macrophage infiltration and steatohepatitis in chronic hepatic injury. Gut 2012;61:416-426.
15) Galastri S, Zamara E, Milani S, Novo E, Provenzano A, Delogu W, Vizzutti F, et al. Lack of CC chemokine ligand 2 differentially affects inflammation and fibrosis according to the genetic background in a murine model of steatohepatitis. Clin Sci (Lond) 2012;123:459-471.
16) Spiegel S, Milstien S. Sphingosine-1-phosphate: an enigmatic signalling lipid. Nat Rev Mol Cell Biol 2003;4:397-407.
17) Schwalm S, Pfeilschifter J, Huwiler A. Sphingosine-1-phosphate: a Janus-faced mediator of fibrotic diseases. Biochim Biophys Acta 2013;1831:239-250.
18) Huang LS, Berdyshev E, Mathew B, Fu P, Gorshkova IA, He D, et al. Targeting sphingosine kinase 1 attenuates bleomycin-induced pulmonary fibrosis. FASEB J 2013;27:1749-1760.
19) Long DA, Price KL. Sphingosine kinase-1: a potential mediator of renal fibrosis. Kidney Int 2009;76:815-817.
20) Gellings Lowe N, Swaney JS, Moreno KM, Sabbadini RA. Sphingosine-1-phosphate and sphingosine kinase are critical for transforming growth factor-beta-stimulated collagen production by cardiac fibroblasts. Cardiovasc Res 2009;82:303-312.

21) Bu S, Asano Y, Bujor A, Highland K, Hant F, Trojanowska M. Dihydrosphingosine 1-phosphate has a potent antifibrotic effect in scleroderma fibroblasts via normalization of phosphatase and tensin homolog levels. Arthritis Rheum 2010;62:2117-2126.
22) Li C, Zheng S, You H, Liu X, Lin M, Yang L, et al. Sphingosine 1-phosphate (S1P)/S1P receptors are involved in human liver fibrosis by action on hepatic myofibroblasts motility. J Hepatol 2011;54:1205-1213.
23) Li C, Jiang X, Yang L, Liu X, Yue S, Li L. Involvement of sphingosine 1-phosphate (SIP)/S1P3 signaling in cholestasis-induced liver fibrosis. Am J Pathol 2009;175:1464-1472.
24) **Yang L**, **Yue S**, Liu X, Han Z, Zhang Y, Li L. Sphingosine kinase/sphingosine 1-phosphate (S1P)/S1P receptor axis is involved in liver fibrosis-associated angiogenesis. J Hepatol 2013; 59:114-123.
25) Xiu L, Chang N, Yang L, Liu X, Ge J, Li L. Intracellular sphingosine 1-phosphate contributes to collagen expression of hepatic myofibroblasts in human liver fibrosis independent of its receptors. Am J Pathol 2015;185:387-398.
26) Yang L, Chang N, Liu X, Han Z, Zhu T, Li C, et al. Bone marrow-derived mesenchymal stem cells differentiate to hepatic myofibroblasts by transforming growth factor-beta1 via sphingosine kinase/sphingosine 1-phosphate (S1P)/S1P receptor axis. Am J Pathol 2012;181:85-97.
27) Tacke F. Targeting hepatic macrophages to treat liver diseases. J Hepatol 2017;66:1300-1312.
28) Ramm GA. Chemokine (C-C motif) receptors in fibrogenesis and hepatic regeneration following acute and chronic liver disease. Hepatology 2009;50:1664-1668.
29) **Marra F**, **Tacke F**. Roles for chemokines in liver disease. Gastroenterology 2014;147:577-594.e571.
30) **Kodama T**, **Takehara T**, Hikita H, Shimizu S, Shigekawa M, Tsunematsu H, et al. Increases in p53 expression induce CTGF synthesis by mouse and human hepatocytes and result in liver fibrosis in mice. J Clin Invest 2011;121:3343-3356.
31) Bataller R, Brenner DA. Liver fibrosis. J Clin Invest 2005;115: 209-218.
32) Bachmann MF, Kopf M, Marsland BJ. Chemokines: more than just road signs. Nat Rev Immunol 2006;6:159-164.
33) **Zamara E**, **Galastri S**, Aleffi S, Petrai I, Aragno M, Mastrocola R, et al. Prevention of severe toxic liver injury and oxidative stress in MCP-1-deficient mice. J Hepatol 2007;46:230-238.
34) Lakner AM, Steuerwald NM, Walling TL, Ghosh S, Li T, McKillop IH, et al. Inhibitory effects of microRNA 19b in hepatic stellate cell-mediated fibrogenesis. Hepatology 2012;56: 300-310.
35) Su S, Zhao Q, He C, Huang D, Liu J, Chen F, et al. miR-142-5p and miR-130a-3p are regulated by IL-4 and IL-13 and control profibrogenic macrophage program. Nat Commun 2015;6: 8523.
36) **Tu X**, **Zhang H**, **Zhang J**, Zhao S, Zheng X, Zhang Z, et al. MicroRNA-101 suppresses liver fibrosis by targeting the TGFbeta signalling pathway. J Pathol 2014;234:46-59.
37) Ozpolat B, Sood AK, Lopez-Berestein G. Nanomedicine based approaches for the delivery of siRNA in cancer. J Intern Med 2010;267:44-53.
38) Hyun J, Wang S, Kim J, Rao KM, Park SY, Chung I, Ha CS, et al. MicroRNA-378 limits activation of hepatic stellate cells and liver fibrosis by suppressing Gli3 expression. Nat Commun 2016;7:10993.

Author names in bold designate shared co-first authorship.

# Supporting Information

Additional Supporting Information may be found at onlinelibrary.wiley.com/doi/10.1002/hep.29885/suppinfo